Article:

Zheng, L. orcid.org/0000-0001-8271-4442, Ji, S. and Zhang, Y. (2018) Lifted and reattached behaviour of laminar premixed flame under external acoustic excitation. Experimental Thermal and Fluid Science, 98. pp. 683-692. ISSN 0894-1777

https://doi.org/10.1016/j.expthermflusci.2018.07.013

Lifted and reattached behaviour of laminar Premixed flame under external acoustic excitation

Lukai Zheng[a*], Shuaida Ji[b], Yang Zhang[b]

[a] Nanjing Institute of Technology, Nanjing 211167, China

[b] University of Sheffield, Sheffield, S20 1AH, United Kingdom

Abstract

The flame chemiluminescent emission fluctuations and the vortex structure of the lifted jet flame under acoustic excitation were studied in this investigation. By employing high-speed visualization and DFCD (Digital Flame Colour Discrimination) image processing method, the fluctuation of the instantaneous mixture fraction has been found highly correlated with the lifted height variations. It has been observed that during the flame drifting to downstream, there is no obvious shifting on the mixture fraction. However, when the flame travels back to upstream, the fuel mixture has been evidently diluted. In addition, the stabilisation mechanism can be further explained by analysing the velocity fluctuation of the vortices in the shear layer via PIV. Measurements show that, the turbulent stretching at the shear layer generated by the excitation leading to the flame lift-off. on the other hand, the Kelvin-Helmholtz vortices in the unburn part play a key role in preventing flame lift-off. But, the excessive external acoustic excitation leads to blow-off due to over dilution and increased lifted height.

Keyword: *Acoustic excitation, Premixed flame, Flame lift-off, Kelvin-Helmholtz vortices.*

[*] Corresponding author E-mail: lukaizheng7@gmail.com (Lukai Zheng); yz100@sheffield.ac.uk (Yang Zhang)

1 Introduction

In most industrial applications, jet flame lifted off is always been regarded as the most undesirable instability problem, as it's unstable and easy to blow-off abruptly. Hence, the stabilization and extinction mechanism have been widely investigated numerically and experimentally.

A non-premixed jet flame has a tendency to lift off from the burner nozzle position when the jet velocity of the flame is over a critical value of U_c [1]. With the increasing of the jet velocity, the lifted height will increase and when it's beyond certain critical height and the flame will be blown off [2]. Therefore, the stability of the lifted flame is an important parameter for basic combustor design. Scholefield and Garside's theory [3] claimed that the transition to turbulence is a prerequisite for the lifted diffusion flame stabilization and the flame anchors at a point where the flow is turbulent. Gollahalli [4] argued that the flame will tend to stable at the position where the local flow velocity balance the normal flame propagation velocity. Navarro-Martinez and Kronenburg [5] have demonstrated that the excessive turbulent stretching at the nozzle leads to the lift-off and they also claimed that auto-ignition can be used to promote the flame stabilization mechanism. Recently the observation from Kiran and Mishra's [2] visual experiment proved the flame lift-off height varies linearly with jet exit velocity. They presented a semi-empirical correlation between the normalized lift-off height to the nozzle exit diameter.

$$\frac{H_L}{D_f} = 1.8 \times 10^{-3} \frac{U_f}{D_f}$$

H_L: lift-off height

D_f: diameter of the fuel tube

U_f: fuel jet velocity

In addition to the velocity effect, The stoichiometric burning on the physical mechanism blowout has been investigated by Broadwell et al. [6] and Pitts [7]. According to their study on diffusion flame, the fresh air entrained by the vortices structure cools down and over dilutes the flame jet, which leads to the flame extinction.

For a lifted flame, it has been shown by many researchers that, the rolling-up processes of vortices structure generated by the bluff body or acoustic perturbation will prevent the lifted flame from propagating downstream [8–12]. Flame response to specific external excitation in the terms of frequency and amplitude was studied theoretically and experimentally by Demare and Baillot [13]. They concluded that secondary vortices are sufficiently powerful to make the flame propagate oppositely. The flame lifting and reattaching characteristics and hysteresis zone where the flame anchoring may occur has been noticed by Gollahall in 1986. [4] The study of diffusion flame stability mechanisms in the hysteresis region by acoustically exciting the unburned components has been investigated by Lin et al.[14] and [9], The most significant effect was found when the acoustic frequency matched the fundamental frequency of the vortex. Chao et al. have demonstrated that, the acoustic excitation at certain frequencies could extend the blowout limit by more than 25% [9]. Moreover, the stability method of acoustic excitation on lifted flame also has been proved to be feasible for soot suppression and emission control[15–17].

On the other hand, Kim et al. [18] and Kartheekeyan et al. [19] have observed that, for premixed flame, the flow oscillation affects the local strain rate at the shear layers, which contributes to the fluctuation of heat release rate and mixing rate. Additionally, the unsteady vorticial structure pass by can stretch and quench the flame[20]. However, the variation of the local fuel to air ration by these vortices cannot be ignored as it will be demonstrated in this study. Chen and Zhang has experimentally investigated the nonlinear coupling characteristics on different equivalence ratios of propane/air flame [21]. It has showed the existence of complex nonlinear frequency components created by the coupling of buoyance driven instability and the acoustic excitation.

While the acoustic excitation has been widely investigated from two aspects: the acoustic stabilization mechanism for diffusion flame and the flame shear layer dynamic experimentally [19,22–26] or numerically [27] for premixed flame. There is lack of the knowledge on the transient dynamics of the lifted and reattached phenomenon for the premixed flame. The present work investigates a conical laminar premixed flame in a rectangular tube excited by acoustic wave. A comprehensive analysis on the premixed flame periodically lifted and reattached phenomenon induced by external acoustic excitation with the combination of diagnostic methods, colour imaging [28], schlieren and PIV methods. The periodical mechanism has been addressed from two aspects: the velocity field of the vorticity at the shear layers and premixed flame stoichiometry burning propagation preference. The Digital Flame Colour Discrimination (DFCD) technique is a unique method to analysis equivalence ratio fluctuation and the transient flame shear layer dynamics. It provides a more intuitive evaluation on the fuel concentration distribution. Combined with the Kelvin-Helmholtz vortex structure observed from the schlieren method, the results provide a good explanation for the flame reattachment progress. The oscillatory behaviour of laminar flame dynamic structure and lifted height are experimentally investigated with time resolved contour line detection method.

2 Experiment setup

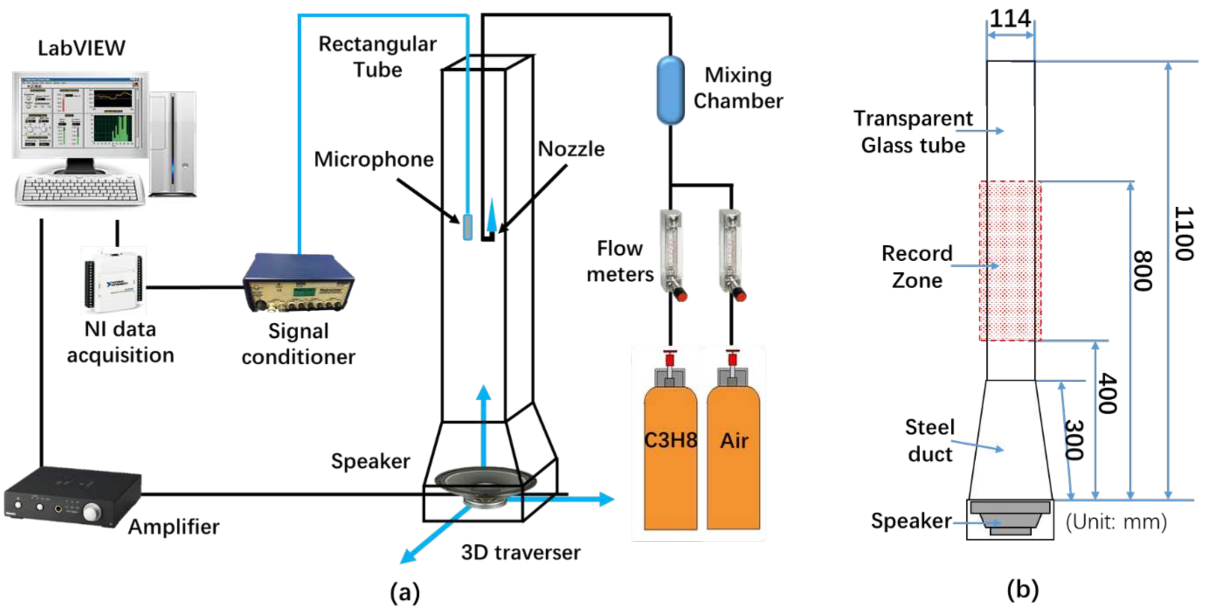

Figure 1. (a) The experimental apparatus; (b) Schematic of the geometry of the square tube and loudspeaker

The schematic of the experimental apparatus is shown in Figure 1 and the actual picture of the setup is shown Figure 2. The experimental setup mainly contains two systems: a burner system and an acoustic generating and sound acquisition system. In the burner system, the gaseous fuel and air are supplied from a propane cylinder and air compressor. The flow rate is controlled by a rotameter. The fuel and air are connected with a mixing chamber to produce a premixed flame at the equivalence ratio of 1.4 (C_3H_8 0.12L/min; Air 2.046L/min). The nozzle position can be adjusted within the top end opened tube, which is made with four glass panels and braced by four steel brackets. The fuel nozzle is customized built, and the main dimensions are listed in the in Figure 2 the unit of mm. The shell of the nozzle can be separated into two parts, named top holder and bottom holder. These two parts are sealed properly when flame on. Inside of the shell, it mainly contains a swirler to stabilize the flame and a honeycomb to smooth the fuel flow.

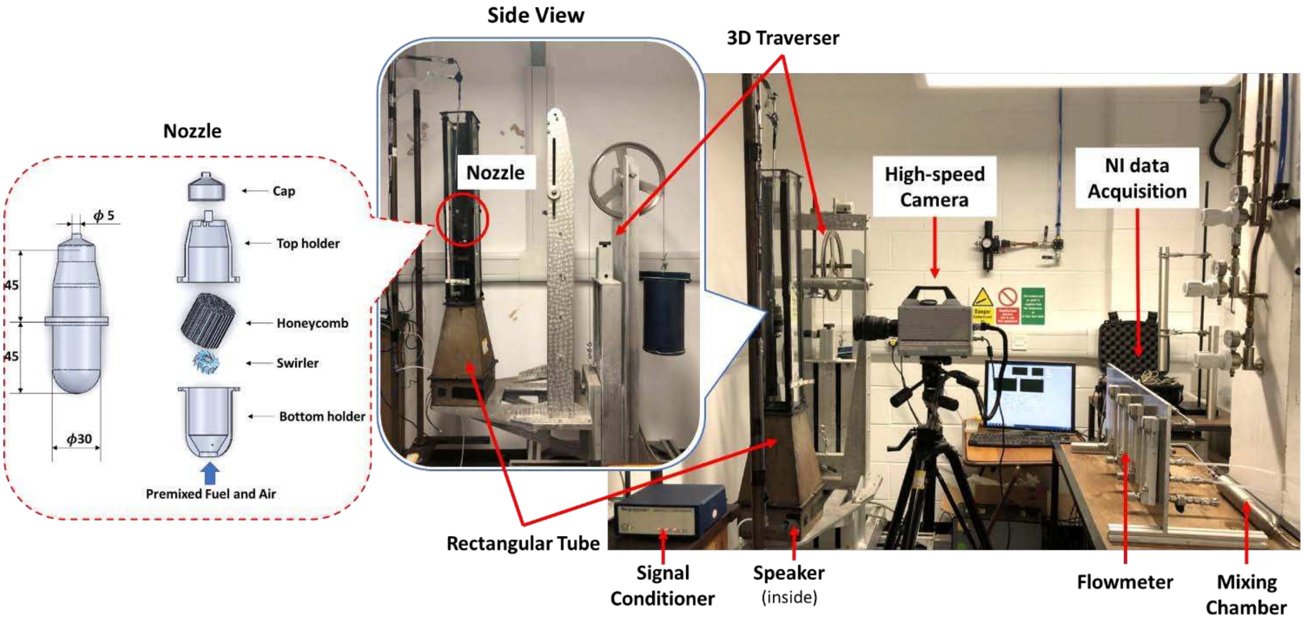

Figure 2 Actual picture of the set-up

The dimensions of the tube are 1100 mm in length and 114 mm in width of the square. A large chamber is deliberately chosen so that the feedback mechanism from the flame itself can be minimised. The details geometry of the square tube is shown in Figure 1 (b). It consists the transparent top tube and steel pyramidal tube at the bottom. As the top end of the tube is open, to avoid the disturbance of the ventilation system in the lab, the nozzle position should keep a certain distance away from the top end. Considering the field of observation and the repeatability, the flame pattern and the sound pressure have been recorded within the range of the tube from 400 mm to 800 mm. The acoustic generator was placed at the bottom end of the tube and fixed on a computer controlled 3-D traverse system. The frequency of the acoustic generating system was controlled by LabVIEW and the output voltage (V) of the amplifier was fixed at 3V. The reading of the sound pressure was collected by a microphone which is mounted at the nozzle and recorded by the National Instruments DAQ card. The measurement uncertainty is presented in Table 1.

Table. 1 Experimental Uncertainty for Control Variables

Measured Quantity	Measured Range	Total Measurement Uncertainty %
Fuel Flowmeter (L/min)	0 – 320	± 3 %
Air Flowmeter (L/min)	0 – 5	± 3 %
Microphone (Pa)	0 – 500	± 1 %
Amplifier (V)	0 – 5	± 1 %
3D Traverser (m)	0-1	± 2%

According the Previous research done by Chen [29], the four resonant frequencies in this duct are 63.61Hz, 218.01Hz, 385.11Hz and 547.71Hz. These results are measured at the room temperature condition without the flame on. The standing wave in the duct can be affected by the temperature and the flame. Therefore, the experimental measurements of the acoustic responses were made along the length of the tube using a microphone with the flame on. The pressure value has been recorded at different position from 400mm to 800mm with 2 mm intervals through the whole tube and the measurement point was in the centre of the tube. The range of excitation frequency was from 20 Hz to 600 Hz in increments of 5 Hz, with a voltage amplitude of 5 V. The experimental observation in Figure 3 indicates that the first four modes of the present rig are 90 Hz, 200 Hz, 380 Hz, and 500 Hz.

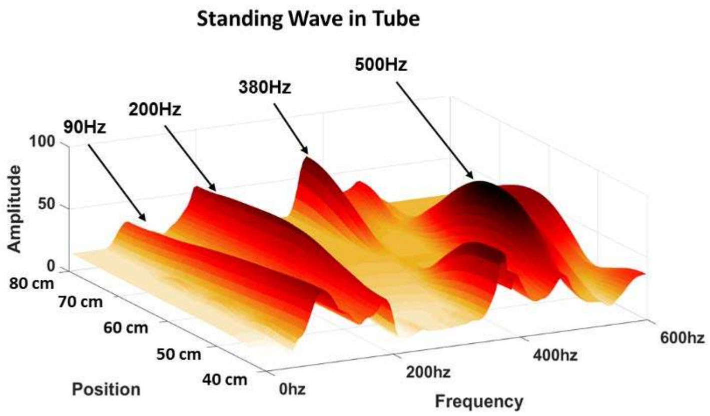

Figure 3 Experimental measurement of pressure response to position and frequency with flame on

The acoustic induced lifted-off behaviour is more evident under the high excitation frequency and high-pressure condition. Hence, the acoustic excitation frequencies of 380 Hz and 500 Hz were set as main frequencies for further investigation.

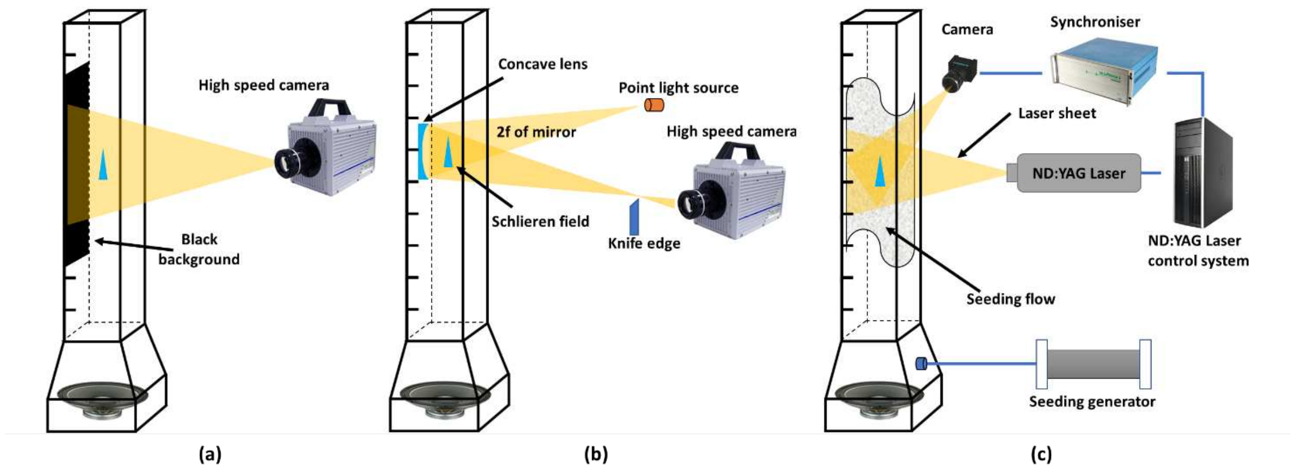

Figure 4 (a) colour imaging recording setup; (b) Schlieren system setup; (C) PIV system setup

The optical record setup consists of a Photron-SA4 high speed colour camera with Sigma zoom 24-70mm lens and the computer control and recording system. Both of the colour and schlieren images were recorded by the high-speed camera at the full frame of 1024×1024 pixels. The colour image recording method is shown in Figure 4 (a). To avoid the background noise signals affecting the weak flame signal detection, the experiments were carried out in a dark room in addition to using black background behind the flame. To ensure the accuracy and generalization, 2000 images were recorded at a shutter speed of 2000 images per second at each condition. The images were analysed by MatLab.

A single mirror schlieren imaging system was applied to visualise the flow dynamics and vortex structure. With this configuration, vortices in the hysteresis region and the self-illuminated flame were both clearly shown in the schlieren images. The setup for schlieren system is shown in Figure 4 (b). It consists of a point light source and one λ/10 parabolic mirror with 75 mm diameter and 75 cm focal length. A knife edge is placed at the focal point, just in front of camera, to adjust the brightness and contrast.

The flow field is measured by a PIV system which consists of a laser sheet generator, a laser pulse synchroniser, a seeding generator, a data acquisition system and data analysis software, shown in Figure 4 (c). A double-pulse ND: YAG laser, operating at a wavelength of 532 nm, a pulse rate of 15 Hz and an energy per pulse of 190 mJ is used in this experiment and it is synchronized with a TSI Powerview^{TM} Plus 4MP Camera used to capture particle images. The Laserpulse Synchroniser model 610035 from TSI is a timing control unit for the PIV applications. It automates control of the timing between laser pulses, camera, camera interfaces and image acquisition. For PIV measurements, these signals are controlled by the synchronizer via Insight 3G data acquisition, analysis and display software. A solid particle generator and average 3 μm titanium dioxide TiO_2 seeding particles are used in this experiment. These seeding particles are injected into the tube with the fuel and air together.

3 Results and Analysis

3.1 Hysteresis Behaviour

Figure 5 (a) presents the sequence of photographs from the single-mirror schlieren setting at an excitation frequency of 380 Hz and forcing intensity of 40 Pa to show the hysteresis region and the self-illuminated flame with shutter speed of 1/50 s at equal intervals. Under the strong excitation, the periodical lifted-off and reattachment process of the premixed flame can be clearly observed in the visible flame area. The motion is concurrent with the activity of the hot gas region.

To obtain a better observation of the flame periodically lifted behaviour, higher shutter speed 1/2000 s has been carried out for the visible flame imaging shown in Figure 5 (b). The samples of series images in successive 4/2000 seconds display the visible flame front structure in transition of lifted-off and reattachment. Under the acoustic forcing, the flame front exhibit severe deformation with evident wrinkle fluctuation, separated flame bubbles and flame base lifted-up.

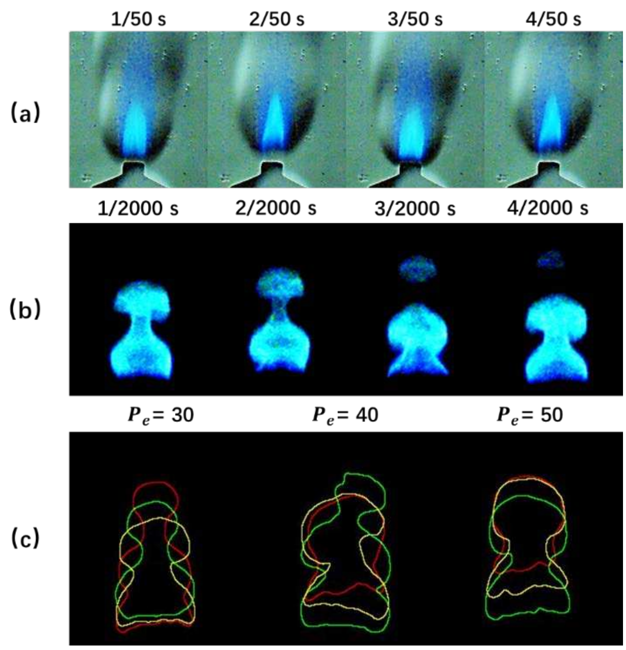

Figure 5 (a) The sequence of photographs from the single-mirror schlieren at a shutter speed of 1/50 s; (b) The samples of successive colour images in 4/2000 seconds; (c) Three sequential samples of the flame front contour lines with 1/2000 s interval

A MatLab based contour detection algorithm has been employed to define the conical flame front and the extracted boundary lines are shown in Figure 5(c). The three sequential samples of the flame front contour lines with 1/2000 s interval from the 380 Hz frequency excitation case are drawn in each of the forcing pressure conditions, 30 Pa, 40 Pa and 50 Pa. The root segment of the front exhibits a noticeable position shifting in the vertical direction. The contour lines illustrate that the fluctuating amplitude of lifted height keeps growing with the increase of the perturbed pressure. In addition, the flame front exhibits an asymmetrically irregular geometry which is similar as what mentioned by Bourehla et al [30] and Gollahalli et al.[4]. These observations demonstrate that the lifted-off behaviour of premixed flame is sensitive to the external excitation. The formation of hysteresis and reattachment processes will be investigated and identified by its dominant flow characteristic in this experimental study.

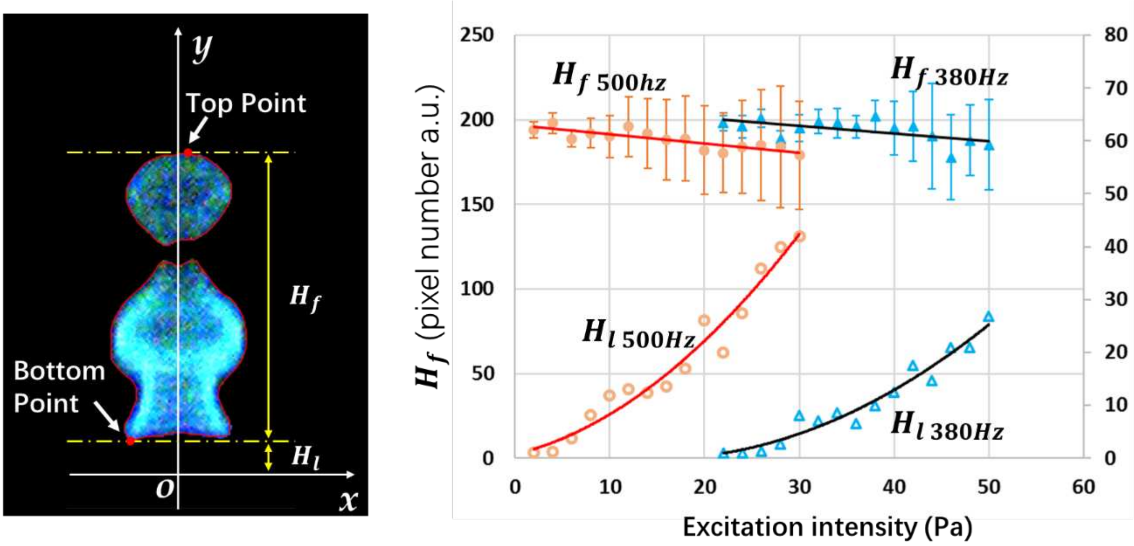

(a) **(b)**

Figure 6 The variation of flame height H_f and lift-off height H_l of acoustically excited flame

The diagrammatic geometry of a 2D flame captured by the high-speed camera at a shutter speed of 1/2000s with the selective colour enhancement technique is shown in Figure 6 (a). The red boundary line of the flame presented the smoothing of the boundary gained through the application of the interpolation points principle. The centre point (0, 0) of the coordinate system is located at the centre of the nozzle exit. The flame length H_f is defined as the non-dimensional distance between the Top Point and the Bottom Point calculated by the number of pixels in the *y* direction, shown Figure 6 (a). The lift-off height H_l is defined by the distance in the *y* direction between the Bottom Point and the nozzle exit. The value of the visible flame length H_f and the lift-off height H_l are the average of 500 selected images for each test case under forcing frequencies of 380 Hz and 500 Hz at different external acoustic forcing intensity, shown in Figure 6 (b). The measurement of sound amplitude ranges from the initial sign of lift-off to blow off point. Therefore, the amplitude ranges for the forcing frequencies 380 Hz and 500 Hz depended on their resistance of blow-off, 22—50 Pa and 2—30 Pa respectively. The flame length H_f exhibits a descending trend for both frequency groups. The error bar presents the standard deviation of flame lengths fluctuation amplitude. As can be obviously noticed from the graph, the external sound pressure promotes the flame length fluctuation. This is mainly contributed by the growing flame lifted height combined with the generation of separated flame bubbles. Moreover, the growing rate of flame lifted height from 500 Hz frequency excitation is higher than that from 380 Hz frequency excitation, which indicated the premixed flame is prone to be disturbed and quenched suddenly under high frequency acoustic perturbation condition. The observation is at variance with the results of the non-premixed flame from Chen[31].

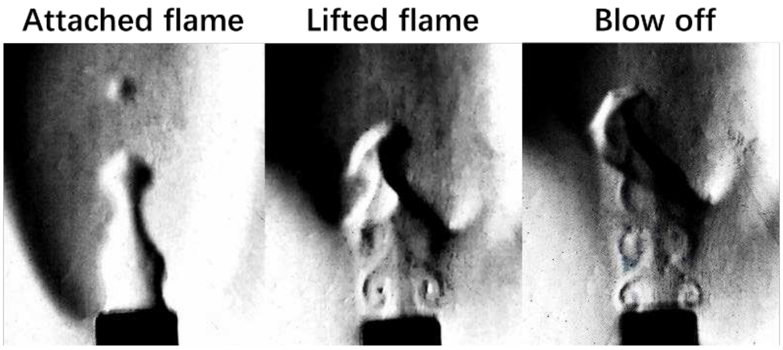

(a) (b) (c)

Figure 7 Sample schlieren pictures for three perturbance conditions

Figure 7 presents the sample schlieren picture at the salient feature point for each of three sound perturbance conditions at 380 Hz, including attached flame (20 Pa), lifted flame (35 Pa) and blow off (50 Pa). Although the vertical orientation of the knife edge is only sensitive to the radial density gradients, the Kelvin-Helmholtz vortex structure become visible on the unburn jet shear layer near the nozzle.

At the low sound amplitude level, the configuration of the flame front presents as a wavy boundary before flame lifted. With the increase of the external perturbation, the waves overturn the vicinity air and grow into billows in the unburning hysteresis region, which leads to the intermittent flame holding. In the burning flame part, the convolutions structure become distorted and gradually dissipated. Because the formation of the vortices structure is subsided as the presence of the flame according to the studies by Gollahalli [4] and Chao [9]. Based on the observation of the massive schlieren pictures, it is shown that the highest stabilized position is most probable at the top of the second pairing of the coherent vortices. The stabilization mechanism of the Kelvin-Helmholtz vortex structure will be further analysed in 3.3 and 3.4. With further increasing the sound pressure level causes the server interference of the surrounding air and fuel. The excessive re-entrained cold fresh air from the vortices cools down the hot products, which results in the reduction in heat release [32] and flame extinction eventually. During the blow-off procedure shown in Figure 7 (c), the organized stream-wise vortices pair gradually spread to larger-scale structure further downstream, which is in accordance with the observation by Demare et al.[11].

3.2 Nonlinear Coupling of Lifted Flame and Acoustic Wave

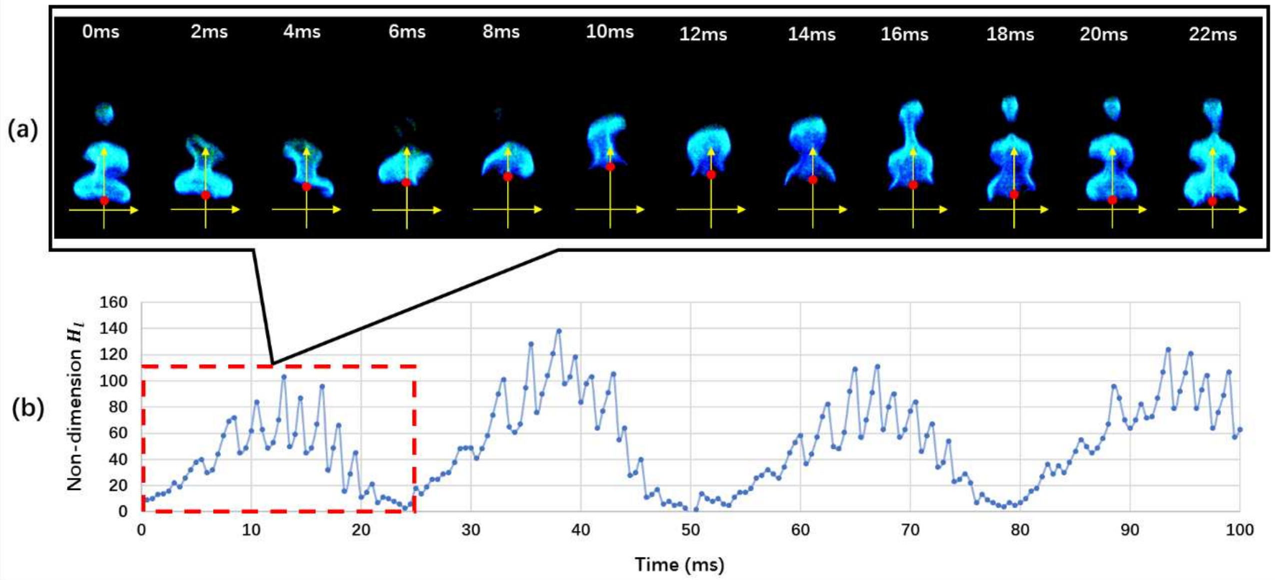

Figure 8 (a) Colour images for circle process the attachment, lift-off and reattachment; (b) The trajectories of the flame lifted height

Figure 8 (a) shows the sequence of the colour images for the flame in the transition circle process of attachment, lift-off and reattachment. The successive frames are at equal interval of 2ms. According to the coordinate system established in Figure 6, the trajectories of the visual flame lifted height, showed in Figure 8 (b), was recorded at 2000 fps in 100ms. As obviously shown in the graph, besides of the oscillations of lifting and reattachment, there was another high frequency oscillation throughout the time.

To determine the principle of the oscillations, FFT analysis was applied to the data of various acoustic intensities from the two frequency cases, shown in Figure 9. The FFT lines graph illustrates the dynamics of lifted height under various acoustic perturbations. The frequency components perform differently at different external excitation frequencies and intensities. Demare and Baillot [11] claimed that the lifted-off height fluctuated randomly despite under the periodic forcing. However, as shown in the results, generally for all the cases, at particular excitation, the single peak of lift-off frequency f_L dominate the flame dynamic can always be detected in the range of 20 Hz to 40 Hz. That indicates, the fluctuation of the lifted height is not random, and it actually correlates to the formation conditions of the Kelvin-Helmholtz vortices and flame burning speed. The excitation frequencies f_e show more evident peaks under the tender acoustic forcing intensity. There is no nature flame flicking frequency can be detected, which indicates the buoyancy driving force doesn't have an effect on the flame lifted fluctuation at this low jet velocity (Re= 557).

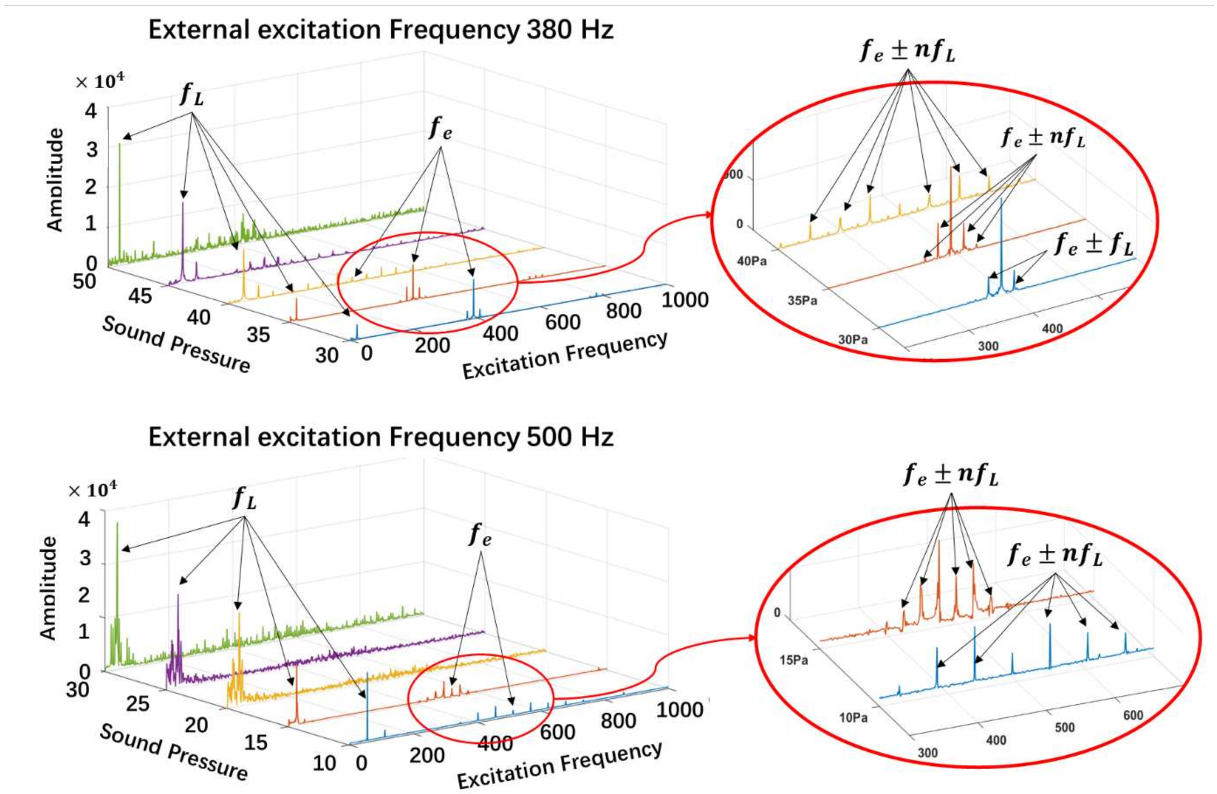

Figure 9 The frequency of the lifted height for various acoustic excitation conditions

At the mild excitation amplitude in both cases of 380 Hz and 500 Hz, the sets of the fore and after peaks that accompany the dominated and harmonic frequencies $f_e \pm nf_L$ have been detected. The sets of accompanied fore and after peaks $f_e \pm nf_L$ are explained by nonlinear coupling theory, which has been reported by Wang [21] recently. The two frequencies components can be simplified into wave signals, shown in below:

$$Y_{Excitation}(t) = x_e \sin(w_e t) \text{ and } Y_{Lifted}(t) = x_L \sin(w_L t);$$

The nonlinear coupling results in the creation of the frequency component as

$$Y_{coupling}(t) = k \sin(w_e t) \sin(w_L t);$$

This can then be broken down into the following equation:

$$Y_{coupling}(t) = \frac{k[\cos(w_e - w_L)\, t] - [\cos(w_e + w_L)\, t]}{2}$$

Hence, this is the mainly explanation for the nonlinear coupling relationship of the $f_e \pm n f_L$.

The stabilization mechanism of the vortices has been reported by many researches [33,34]. The researchers noticed that, for the lifted flame, at the hysteresis region, the vortices play an important role for the flame stabilization and reattachment. Therefore, in the following paragraph the phenomenon of acoustic induced lifted flame propagation procedure will be analysed mainly from two aspects: the velocity and vorticity field with PIV measurement and the flame propagation preference based on flame chemiluminescence detection.

3.3 PIV measurements

It's well-known that when the jet velocity U_{jet} larger than the burning velocity U_{burn}, the flame detaches itself from the nozzle and stabilizes at the where $U_{jet} \approx U_{burn}$ in the downstream. The lifted height is unstable, as the hysteresis zone is vulnerable to the external interference. PIV has been applied to measure the velocity distribution of the jet with or without the vortices.

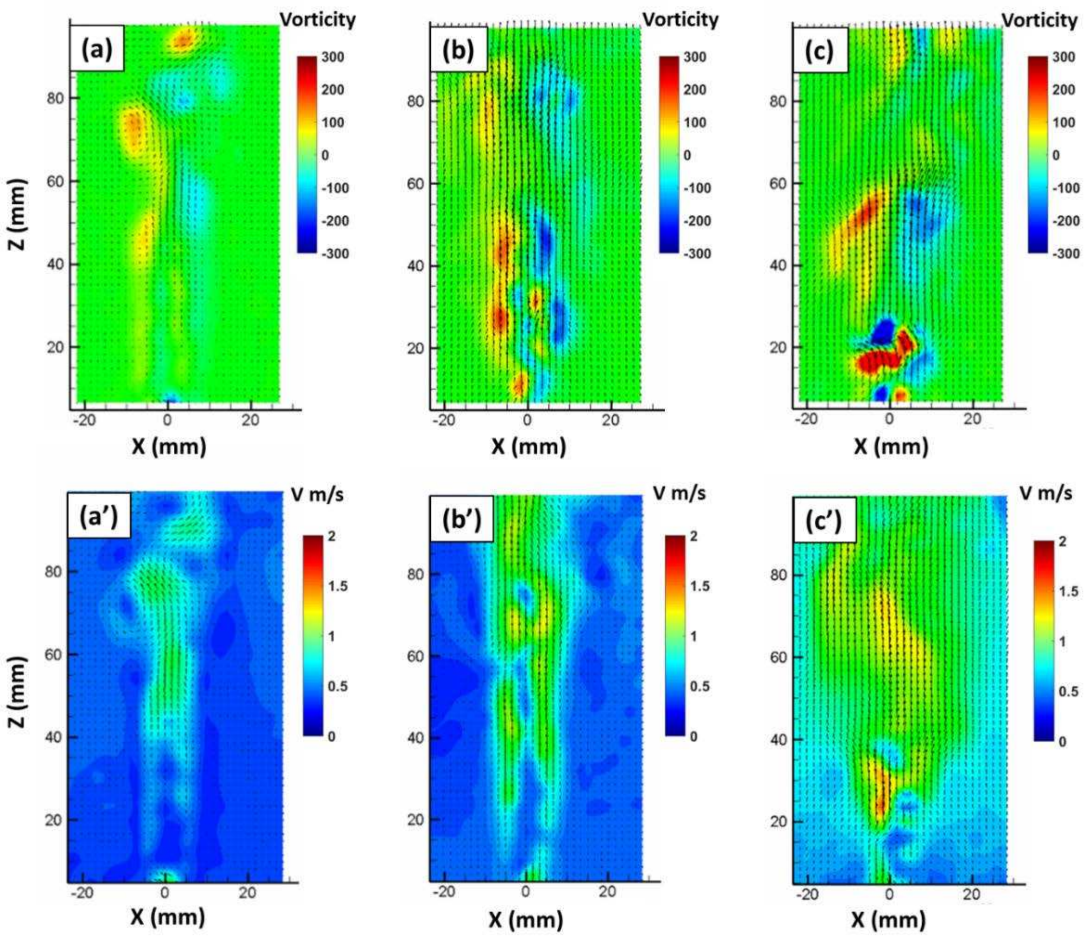

Figure 10. Velocity vectors and the vorticity contour maps of the instantaneous propane–air flame flow at the excitation frequency of 380Hz.

The contour maps of the velocity and vorticity for the premixed flame flow field under 380 Hz have been plotted in Figure 10. Three perturbance flame features induced by three sound intensities excitation levels have been investigated. Flame without excitation (a & a'), excited attached flame (b & b') and excited lifted flame (c and c') are shown from left to right in Figure 10. Under the external excitation condition, both of the fuel jet and the ambient air are disturbed by the acoustic wave. With the increase of the sound amplitude, the more obvious disturbance has been shown in the maps, especially for the area near the nozzle position at the coordination (0,0). From the plots of (a') and (b'), it's very interesting to notice that, before the flame lifted off, the velocity of the fuel jet at the upstream is smaller comparing with the ambient air and the relative velocity at the flame shear layer has been enlarged with the increase of the sound amplitude. Along the downstream, the air flow motion of the hot gas above the flame gradually further accelerates due to the buoyancy effect. Therefore, further increasing the acoustic disturbance until the relative velocity at the shear layer reaches the critical value U_c, and then the jet flame starts to lift off.

Contrary to the mild excited case, after the flame lifted-off, the relative velocity field condition reversed, the velocity of unburned jet flow is much larger than that of the ambient air and the velocity disparity results in the formation of Kelvin-Helmholtz vortices, which has been clear illustrated in (c). There is much more intensive vorticity region concentrated above the nozzle. According to its corresponding velocity map in (c'), at the Kelvin-Helmholtz rolling up region, there are obvious downward velocity vectors in the flow pattern. This observation is matched with Chao's [9] and Demare's [13] result. Chao et cl. claimed that the local velocity of the vortex core region is higher than the nature jet, but the outer edge of the layer and the mean velocity of the travelling wave has been dramatically decreased. Therefore, the rolling-up vortices effectively prevent the lifted flame from propagation upstream. Demare and Baillot presented velocity field of both the vertical and the horizontal views. They found that the vortex radial velocity of the excited jet is nearly half of the natural jet and the root-mean-square value is 25% lower [11]. Therefore, the Kelvin-Helmholtz ring structure provides a suitable circumstance for the flame reattachment. Moreover, these vortex structures not only minimise the velocity disparity at the shear layer, but also promote the further mixing between the fuel and the ambient air. The mixture fraction will be further analysed by the DFCD image processing method on the flame chemiluminescence.

3.4 Flame Chemiluminescence

The experimental data measured by Gu [35] proved that burning velocity for premixed flame reaches its maximum value when the equivalence ratio is around 1. In addition, Walchshofer has concluded that the lifted flame is stabilized close to the surface stoichiometric mixing conditions [36]. In another word, the premixed flame at equivalence ratio 1.4 preferably drifts towards the relatively fuel leaner side. Many modelling works on premixed flame dynamics attempt to calculate the equivalence ratio fluctuation response to imposed acoustic excitation [37–39]. The recent experimental work by Kartheekeyan and Chakravarthy [19] only presented a blurry configuration of the chemiluminescence images. The acoustic induced dilution behaviour can be quantitatively analysed with DFCD, which has been implemented in the present work for evaluating the distribution of fuel concentration. This method has been introduced in Huang's previous researches [28] and applied on both of gaseous [40] and liquid combustions [41].

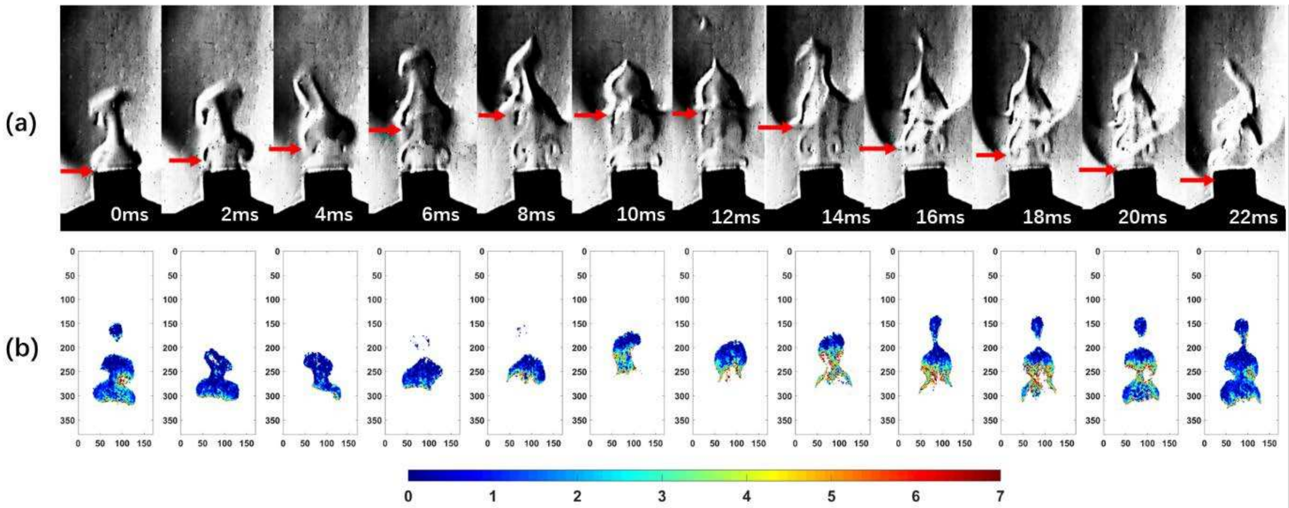

Figure 11 (a) The schlieren images for flame and jet flow structure during the lifted and reattached process; (b) Instantaneous calculated CH*/C2* ratio colour map

the CH*/C2* ratio has been proved to have monotonic relation with the equivalence ratio. It can be regarded as an indicator to reveal the fuel mixing fraction level, in which the fuel lean flame has higher CH*/C2* ratio and high fuel concentration flame has lower CH*/C2* ratio. Figure 11 (a) shows the sequence of the schlieren images for the flame lifted and reattached circle process with 2 ms intervals. The Kelvin-Helmholtz rolling-up structure can be clearly recognized in the unburnt jet region above the nozzle when the flame lifted. Figure 11 (b) presents the instantaneous colour map of the calculated CH*/C2* ratio of the corresponding images. The ratio ranges from 0 to 7 and displays the colour from dark blue to red. During the flame propagating downstream, the flame area gradually decreases, but there is no evidence change in the fuel concentration and most of the flame area exhibited as dark blue. As soon as the flame lifted to the highest position, the reddish and yellowish colour gradually emerge at the bottom section, which indicates the vortex-up configuration enhances the mixing between the fuel and the surrounding air. During the falling period, the lifted flame propagates upstream as a result of vortices induced local lower mixture fraction, which is consistent with flame propagation preference. It's also worth noticing that, beside of the predominant distribution zone of the reddish and yellowish points at the bottom region of the flame, it also occurs at the core of the vortex. Therefore, based on all the discussion above, the upstream propagation behaviour of the acoustic excited lifted flame could be explained by rolling-up vortices stabilization mechanism and local mixing enhancement.

4. Conclusion

This study has presented a quantitative experimental observation on the acoustic excitation induced lifted flame. The investigated lifted flame features include fluctuation of flame length and lifted height, velocity field of the vortex structure, premixed flame fuel/air mixing ratio and propagation behaviour. It has been observed that:

- The premixed flame is prone to be disturbed and can extinct suddenly under high frequency acoustic perturbation condition. The fluctuating amplitude of lifted height keeps growing with the increase of the forcing intensity. The flame blows off at 380 Hz/50 Pa and 500 Hz/30 Pa in this case.
- The external forcing pressure promotes the flame height fluctuation due to the appearance of the separated flame pocket. The growing rate of flame lifted height from 500 Hz frequency excitation is higher than that from 380 Hz frequency excitation
- Kelvin-Helmholtz ring structure forms at the unburn jet boundary near the nozzle when flame lifted, which can intermittently stabilize the flame. But the flame will blow off eventually under the severe turbulence stretching due to the excessive re-entrainment of cold fresh air to cool down the hot products and the flame fails to sustainable.
- Under the low forcing sound pressure, the non-constant value of lift-off frequency f_L has non-linear coupling with the external excitation frequencies f_e, exhibited as $f_e \pm nf_L$. while as,

under the high forcing sound pressure, the vortices dominated the lifted height oscillation with frequency f_L.

- Before flame lifted, relative velocity at the flame shear layer has been enlarged with the increase of the sound amplitude; After the flame lifted, intensive vorticity region concentrated at the Kelvin-Helmholtz rolling up region, which minimises the velocity disparity and provides a suitable circumstance for the flame reattachment.
- During the flame propagating upstream, the CH^*/C_2^* ratio are significant increase at the bottom area. Because, the moderate fresh air entrainment with Kelvin-Helmholtz vortices structure dilutes the mixture fraction. The premixed flame burning speed and propagation preference drag the flame back to the nozzle.

References

[1] D. Demare, F. Baillot, The role of secondary instabilities in the stabilization of a nonpremixed lifted jet flame, Phys. Fluids. 13 (2001) 2662–2670. doi:10.1063/1.1386935.

[2] D.Y. Kiran, D.P. Mishra, Experimental studies of flame stability and emission characteristics of simple LPG jet diffusion flame, Fuel. 86 (2007) 1545–1551. doi:10.1016/j.fuel.2006.10.027.

[3] D.A. Scholefield, J.E. Garside, The structure and stability of diffusion flames, in: Symp. Combust. Flame, Explos. Phenom., Elsevier, 1948: pp. 102–110.

[4] S.R. Gollahalli, Ö. Savaş, R.F. Huang, J.L. Rodriquez Azara, Structure of attached and lifted gas jet flames in hysteresis region, Symp. Combust. 21 (1988) 1463–1471. doi:10.1016/S0082-0784(88)80379-5.

[5] S. Navarro-Martinez, A. Kronenburg, Flame stabilization mechanisms in lifted flames, Flow, Turbul. Combust. 87 (2011) 377–406.

[6] J.E. Broadwell, W.J.A. Dahm, M.G. Mungal, Blowout of turbulent diffusion flames, Symp. Combust. 20 (1985) 303–310. doi:10.1016/S0082-0784(85)80515-4.

[7] W.M. Pitts, Assessment of theories for the behavior and blowout of lifted turbulent jet diffusion flames, Symp. Combust. 22 (1989) 809–816. doi:10.1016/S0082-0784(89)80090-6.

[8] S. Chaudhuri, S. Kostka, M.W. Renfro, B.M. Cetegen, Blowoff dynamics of bluff body stabilized turbulent premixed flames, Combust. Flame. 157 (2010) 790–802. doi:10.1016/j.combustflame.2009.10.020.

[9] Y.-C. Chao, J. Ming-Shan, Behavior of the lifted jet flame under acoustic excitation, Symp. Combust. 24 (1992) 333–340. doi:10.1016/S0082-0784(06)80044-5.

[10] F. Baillot, D. Demare, Physical Mechanisms of a Lifted NonPremixed Flame Stabilized in an Acoustic Field, Combust. Sci. Technol. 174 (2002) 73–98. doi:10.1080/713713066.

[11] D. DEMARE, F. BAILLOT, Acoustic enhancement of combustion in lifted nonpremixed jet flames, Combust. Flame. 139 (n.d.) 312–328. http://cat.inist.fr/?aModele=afficheN&cpsidt=16363812 (accessed February 23, 2017).

[12] J. Oh, Q.S. Khan, Y. Yoon, Acoustic excitation effect on NOx reduction and flame stability in a lifted non-premixed turbulent hydrogen jet with coaxial air, Fuel. 89 (2010) 1492–1498. doi:10.1016/j.fuel.2009.10.001.

[13] D. Damare, F. Baillot, The role of secondary instabilities in the stabilization of a nonpremixed lifted jet flame, Phys. Fluids. 13 (2001) 2662–2670. doi:10.1063/1.1386935.

[14] C.K. Lin, M.S. Jeng, Y.C. Chao, The stabilization mechanism of the lifted jet diffusion flame in the hysteresis region, Exp. Fluids Exp. Methods Their Appl. to Fluid Flow. 14 (1993) 353–365. doi:10.1007/BF00189494.

[15] M. Kim, Y. Choi, J. Oh, Y. Yoon, Flame-vortex interaction and mixing behaviors of turbulent non-premixed jet flames under acoustic forcing, Combust. Flame. 156 (2009) 2252–2263. doi:10.1016/j.combustflame.2009.08.004.

[16] J. Oh, Q.S. Khan, Y. Yoon, Nitrogen dilution effect on flame stability in a lifted non-premixed turbulent hydrogen jet with coaxial air, Fuel. 89 (2010) 1492–1498. doi:10.1016/j.fuel.2009.10.001.

[17] Y. Chao, D. Wu, C. Tsai, Effects of Acoustic Excitation on the Combustion and Pollution Emission Characteristics of a Jet Flame, 0 (2000) 1–13.

[18] K.T. Kim, J.G. Lee, B.D. Quay, D.A. Santavicca, Response of partially premixed flames to acoustic velocity and equivalence ratio perturbations, Combust. Flame. 157 (2010) 1731–1744. doi:10.1016/j.combustflame.2010.04.006.

[19] S. Kartheekeyan, S.R. Chakravarthy, An experimental investigation of an acoustically excited laminar premixed flame, Combust. Flame. 146 (2006) 513–529. doi:10.1016/j.combustflame.2006.04.014.

[20] J.S. Kistler, C.J. Sung, T.G. Kreut, C.K. Law, M. Nishioka, Extinction of counterflow diffusion flames under velocity oscillations, in: Symp. Combust., Elsevier, 1996: pp. 113–120.

[21] Q. Wang, H.W. Huang, H.J. Tang, M. Zhu, Y. Zhang, Nonlinear response of buoyant diffusion flame under acoustic excitation, Fuel. 103 (2013) 364–372. doi:10.1016/j.fuel.2012.08.008.

[22] N. Karimi, M.J. Brear, S.H. Jin, J.P. Monty, Linear and non-linear forced response of a conical, ducted, laminar premixed flame, Combust. Flame. 156 (2009) 2201–2212. doi:10.1016/j.combustflame.2009.06.027.

[23] D.H. Shin, T. Lieuwen, Flame wrinkle destruction processes in harmonically forced, laminar premixed flames, Combust. Flame. 159 (2012) 3312–3322. doi:10.1016/j.combustflame.2012.06.015.

[24] A. Cuquel, D. Durox, T. Schuller, Comptes Rendus Mecanique Impact of flame base dynamics on the non-linear frequency response of conical flames, Comptes Rendus Mec. 341 (2013) 171–180. doi:10.1016/j.crme.2012.11.004.

[25] H.Y. Wang, C.K. Law, T. Lieuwen, Linear response of stretch-affected premixed flames to flow oscillations, Combust. Flame. 156 (2009) 889–895. doi:10.1016/j.combustflame.2009.01.012.

[26] N. Karimi, Response of a conical, laminar premixed flame to low amplitude acoustic forcing - A comparison between experiment and kinematic theories, Energy. 78 (2014) 490–500. doi:10.1016/j.energy.2014.10.036.

[27] S. Schlimpert, M. Meinke, W. Schröder, Nonlinear analysis of an acoustically excited laminar premixed flame, Combust. Flame. 163 (2016) 337–357. doi:10.1016/j.combustflame.2015.09.035.

[28] H.W. Huang, Y. Zhang, Imaging based chemiluminescence characterisation of partially

premixed syngas flames through DFCD technique, Int. J. Hydrogen Energy. 38 (2013) 4839–4847. doi:10.1016/j.ijhydene.2013.01.142.

[29] L. Chen, A theoretical and experimental study on flow characterisation in an acoustically excited chamber, Wave Motion. 58 (2015) 68–76. doi:10.1016/j.wavemoti.2015.07.003.

[30] A. Bourehla, F. Baillot, Appearance and stability of a laminar conical premixed flame subjected to an acoustic perturbation, Combust. Flame. 114 (1998) 303–318. doi:10.1016/S0010-2180(97)00323-4.

[31] L.W. Chen, Y. Zhang, Experimental observation of the nonlinear coupling of flame flow and acoustic wave, Flow Meas. Instrum. 46 (2015) 12–17. doi:10.1016/j.flowmeasinst.2015.09.001.

[32] D.M.H.-P.& K.C.S. E. GUTMARK , T. P. PARR, Stabilization of a Premixed Flame by Shear Flow Excitation, Combust. Sci. Technol. 73 (1990) 521–535. doi:10.1080/00102209008951668.

[33] A. Onder, J. Meyers, Modification of vortex dynamics and transport properties of transitional axisymmetric jets using zero-net-mass-flux actuation, Phys. Fluids. 26 (2014). doi:10.1063/1.4890242.

[34] J. Lee, S.H. Won, S.H. Jin, S.H. Chung, Lifted flames in laminar jets of propane in coflow air, Combust. Flame. 135 (2003) 449–462. doi:10.1016/S0010-2180(03)00182-2.

[35] X.J. Gu, M.Z. Haq, M. Lawes, R. Woolley, Laminar burning velocity and Markstein lengths of methane–air mixtures, Combust. Flame. 121 (2000) 41–58. doi:10.1016/S0010-2180(99)00142-X.

[36] C. Walchshofer, H. Steiner, Computational investigation of the stability of a lifted strongly buoyant jet flame, Combust. Flame. 162 (2015) 613–627. doi:10.1016/j.combustflame.2014.09.007.

[37] T. Lieuwen, Modeling Premixed Combustion-Acoustic Wave Interactions: A Review, J. Propuls. Power. 19 (2003) 765–781. doi:10.2514/2.6193.

[38] J.H. Cho, T. Lieuwen, Laminar premixed flame response to equivalence ratio oscillations, Combust. Flame. 140 (2005) 116–129. doi:10.1016/j.combustflame.2004.10.008.

[39] Shreekrishna, S. Hemchandra, T. Lieuwen, Premixed flame response to equivalence ratio perturbations, Combust. Theory Model. 14 (2010) 681–714. doi:10.1080/13647830.2010.502247.

[40] J. Yang, F.M.S. Mossa, H.W. Huang, Q. Wang, R. Woolley, Y. Zhang, ScienceDirect Oscillating flames in open tubes, Proc. Combust. Inst. 35 (2015) 2075–2082. doi:10.1016/j.proci.2014.07.052.

[41] L. Zheng, A. Faik, Y. Zhang, Flame colour analysis for the droplet combustion of water-in-diesel emulsions, in: 12th Int. Conf. Heat Transf. Fluid Mech. Thermodyn., Malaga, Spain, 2016: pp. 212–217. https://edas.info/web/hefat2016/titles.html#F.